Cross-Polarization Schemes for Improved Heteronuclear Transfers Involving Labile Protons in Biomolecular Solution NMR

How to cite: *Angew. Chem. Int. Ed.* **2023**, *62*, e202304900
doi.org/10.1002/anie.202304900

NMR Spectroscopy

Cross-Polarization Schemes for Improved Heteronuclear Transfers Involving Labile Protons in Biomolecular Solution NMR

*Jihyun Kim, J. Tassilo Grün, Mihajlo Novakovic, Eriks Kupce, Rina Rosenzweig, and Lucio Frydman**

Abstract: INEPT-based experiments are widely used for $^{1}H\rightarrow^{15}N$ transfers, but often fail when involving labile protons due to solvent exchanges. J-based cross polarization (CP) strategies offer a more efficient alternative to perform such transfers, particularly when leveraging the $H^{water}\leftrightarrow H^{N}$ exchange process to boost the $^{1}H\rightarrow^{15}N$ transfer process. This leveraging, however, demands the simultaneous spin-locking of both H^{water} and H^{N} protons by a strong ^{1}H RF field, while fulfilling the $\gamma_H B_{1,H} = \gamma_N B_{1,N}$ Hartmann-Hahn matching condition. Given the low value of γ_N/γ_H, however, these demands are often incompatible—particularly when experiments are executed by the power-limited cryogenic probes used in contemporary high field NMR. The present manuscript discusses CP alternatives that can alleviate this limitation, and evaluates their performance on urea, amino acids, and intrinsically disordered proteins. These alternatives include new CP variants based on frequency-swept and phase-modulated pulses, designed to simultaneously fulfill the aforementioned conflicting conditions. Their performances vis-à-vis current options are theoretically analyzed with Liouville-space simulations, and experimentally tested with double and triple resonance transfer experiments.

Introduction

Biomolecular NMR experiments often demand enhancing the sensitivity of low-γ nuclei by polarization transfers from protons, as well as using polarization transfers to correlate different nuclear species with one another.[1–6] Both the sensitivity enhancing and the multinuclear correlation aspects of these polarization transfers play central roles in tackling the structures and dynamics of proteins and nucleic acids, and often involve bonded $^{1}H/^{15}N$ spin pairs belonging to amide, amine, or imino groups.[6–8] These polarization transfers are usually achieved by a series of pulses and RF-free evolution periods, as in the INEPT pulse block used in ^{1}H–^{15}N HSQC experiments.[9] Here, 90° and 180° hard pulses with suitably interspersed free-evolution delays convert the initial longitudinal proton magnetization H_z to either single- or two-spin operators containing N_x elements, via the conversion of initial states into multi-spin $2H_{\pm}N_z$ intermediates. This kind of transfers, however, may suffer considerable losses in the presence of fast solvent exchanges, as under these conditions the transverse multi-spin components will rapidly decohere by interchanges with the H_z^{water} magnetization. It has been shown that, in such instances, polarization transfers via J-driven cross-polarization—so-called J-CP—can serve as a more robust scheme for transferring polarization from labile protons to heteronuclei.[10–12] As INEPT, CP also proceeds from single-spin proton (H_x^N) to single-spin nitrogen (N_x) polarization via two-spin elements.[13,14] Unlike what happens in INEPT, however, this transfer is gradual and continuous. Hence, if the CP ^{1}H spin-locking field is designed strong enough to capture both the $^{1}H^{N}$ and $^{1}H^{water}$ states, exchange-driven transfers from H_x^{water} to H_x^N can be leveraged to further boost the heteronuclear polarization transfer process. It has thus been shown that even when solvent exchange rates k_{ex} are much larger than the heteronuclear J couplings, the $H_x^N\rightarrow N_x$ CP process can proceed nearly to completion if given long enough contact times.[15] Such CP strategies can then be used to improve the sensitivity of protein 2D NMR experiments, by replacing the

[*] J. Kim, J. T. Grün, M. Novakovic, L. Frydman
Department of Chemical and Biological Physics, Weizmann Institute of Science
Rehovot 7610001 (Israel)
E-mail: lucio.frydman@weizmann.ac.il
J. T. Grün
Current address: BASF SE, RGA/AS—B 009
67056 Ludwigshafen am Rhein (Germany)
M. Novakovic
Current address: Institute of Biochemistry, Department of Biology, ETH Zürich
Hönggerbergring 64, 8093 Zürich (Switzerland)
E. Kupce
Bruker Ltd.
Banner Lane, Coventry CV4 9GH (UK)
R. Rosenzweig
Department of Chemical and Structural Biology, Weizmann Institute of Science
Rehovot 7610001 (Israel)

initial $H_x^N \rightarrow N_x$ INEPT-based transfer with a Hartmann-Hahn (HH) contact block.[16]

CP's ability to execute polarization transfers even under fast $k_{ex} \gg J$ exchanges demands that the labile and water ^{1}Hs be simultaneously spin-locked, while fulfilling the HH match.[17] This demand can be difficult or impossible to fulfill in bioNMR experiments, where the use of high fields leads to large $^1H^N$–$^1H^{water}$ chemical shift differences, and the use of cryogenically-cooled probes limits the γB_1 fields that can be achieved on the low-frequency channels. For the particular setup to be considered here, the maximum safe ^{15}N field that can be deposited without causing RF arcing is $\gamma_N B_{1,N}/2\pi \leq 3.5$ kHz; the HH $\gamma_H B_{1,H} = \gamma_N B_{1,N}$ condition thus requires setting the ^{1}H RF $\gamma_H B_{1,H}/2\pi$ to $\approx$3.5 kHz, a field that is insufficient for providing an effective, simultaneous spin-locking of the water and amide/amine/imino resonances. Paradoxically, considerably stronger $\gamma_H B_{1,H}$ fields are achievable in high-field cryogenically-cooled probes, but these are incompatible with the HH-imposed demands.

A similar scenario, where a strong $\gamma_H B_{1,H}$ field is needed for efficient spin-locking but these strengths cannot be matched by the low-γ RF field hardware, arose decades ago in solid-state NMR.[18] Strong RF fields are then needed on the ^{1}Hs because of the substantial $T_{1\rho}$ shortening arising when $\gamma_H B_{1,H}$ was smaller than the dipolar ^{1}H line width,[19] but these strong fields are hard to match for the low-γ frequency channels. Although these problems were to some extent superseded by the advent of small-diameter magic-angle-spinning coils,[20] a number of experiments were proposed to alleviate these conflicting demands. The present study explores and adapts some of these experiments to the optimization of $^1H^N \rightarrow ^{15}N$ transfers in aqueous systems. We find that the polarization transfer efficiencies of these adapted experiments are comparable to that of current J-CP Schemes under slow exchange and on-resonance irradiation conditions, but they act over broader ^{1}H chemical shift ranges and retain their efficiencies as the solvent exchange rates become faster. These performances are experimentally verified on small biomolecules, on rapidly exchanging lysine protein side chains, and on intrinsically disordered protein (IDP) samples, in a series of tests that also included $^1H \rightarrow ^{15}N \rightarrow ^{13}C$ transfer experiments.[21]

Results and Discussion

Figure 1 summarizes the various pulse sequences explored in this study. They include: (a) CP sequences based on continuous wave (CW) irradiations on all channels with fields applied on resonance at the highest $\gamma_H B_{1,H} = \gamma_N B_{1,N}$ conditions possible, or with the ^{15}N spin-lock applied off-resonance in order to carry out the HH match at a higher $\gamma_N B_{eff,N} = \sqrt{(\gamma_N B_{1,N})^2 + \Delta\Omega_N}$ effective field as aided by the $\Delta\Omega_N$ offset (which can then be matched by the ^{1}H channel thanks to the faster nutation rates achievable in the latter). (b) Phase-modulated schemes based on widely used offset-compensated DIPSI spin-locking pulses,[22] or on a mismatch-optimized I–S transfer MOIST proposal,[23] fulfilling either $\gamma_H B_{1,H} = \gamma_N B_{1,N}$ RF as limited by the probe-imposed maximum $\gamma_N B_{1,N}$, or exploiting off-resonance $\Delta\Omega_N$ effects. (c) A novel CP scheme that we propose based on looped, wideband, uniform rate, smoothly truncated (WURST) ^{1}H pulses, capable of preserving both the H^N and H^{water} magnetizations spin-locked over large chemical shift bandwidths, while still fulfilling the $\gamma_H B_{1,H} = \gamma_N B_{1,N}$ condition. (d) Time-

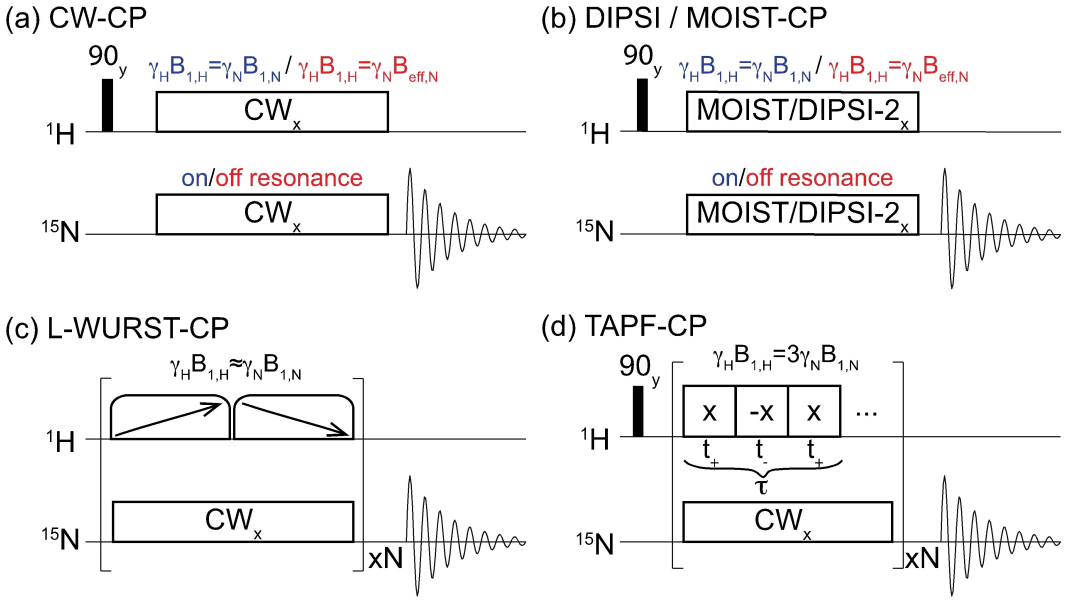

Figure 1. Schematics of the eight CP pulse sequence variants assayed in this work. These included (a) CW-CP with the ^{15}N RF applied on- and off-resonance. (b) Idem but with the RF fields phase modulated according to DIPSI-2 or MOIST schemes to compensate for RF imperfections. (c) A looped WURST-CP sequence based on trains of broadband adiabatic swept pulses chirped in opposite directions. (b) TAPF-CP, a sequence achieving HH match while using n-fold stronger ^{1}H RF fields than conventional CP (in this case, $n = 3$).

averaged precession frequency (TAPF) CP schemes,[24] which can match larger $\gamma_H B_{1,H}$ fields to lower $\gamma_N B_{1,N}$ by unbalanced alternations of the ^1H spin-locking phase.

To the best of our knowledge, the last two sequences are new within the context of solution state NMR, and hence deserve a short explanation. The TAPF scheme was designed to match the large $\gamma_H B_{1,H}$ needed for an effective solid state spin-lock with the lower γB_1 fields achievable by low-γ nuclei like ^{15}N, while still retaining an effective $<\gamma_H B_{1,H}>=\gamma_N B_{1,N}$ HH match. This is carried out by imposing an uneven 180° alternation in the phase of the ^1H spin-locking field $B_{1,H}(t)$, which per unit duration τ applies the ^1H RF with a phase +x for a time τ_+ and with a phase -x for a time τ_-. For sufficiently short overall cycle times τ, the ensuing ^1H field becomes then effectively scaled by a factor $\kappa=(\tau_+-\tau_-)/\tau$. In the present study, we relied on a cycle whose unit involved a +x/-x/+x phase alternation with each phase of an equal $t_+ = t_-$ duration; this lead to a total unit lasting a total time $\tau=2\,t_+ + t_-$, and to a $\kappa=(2\,t_+ - t_-)/(2\,t_+ + t_-)=1/3$ scaling. This allowed us to apply ≈10 kHz for the ^1H spin-locking, while matching ^{15}N fields of ≈3.3 kHz while fulfilling the HH condition.

The second novel scheme, L-WURST CP, is also inspired by a solid-state NMR experiment: broadband adiabatic inversion CP (BRAIN-CP).[25] Whereas in BRAIN-CP, the swept pulses are applied on the low-γ nuclei in order to polarize them while covering large bandwidths associated to anisotropies that are much larger than γB_1, these pulses are here applied on the ^1H channel. Their aim is thus not to receive polarization, but rather to ensure the spin-locking of both $^1H^N$ and $^1H^{water}$ magnetizations throughout the CP process—despite using RF fields set to match ≈ $\gamma_N B_{1,N}$ that would be too weak to achieve a normal ^1H spin-lock. These ^1H pulses, however, are chosen here as adiabatic sweeps with a WURST shape,[26] that can then spin-lock magnetizations along a wide range of targeted ^1H chemical shift offsets. As these swept pulses will only transiently fulfill the HH condition, the efficiency of the polarization transfer —particularly in the presence of exchanges—will be relatively low. To compensate for this, the sequence relies on looping the WURST pulses multiple times, while sweeping the RF in opposite directions. By repeating *N* times this RF-driven sweeps of the H^N and H^{water} magnetizations from the +z direction and back, this sequence takes advantage of a flux of spin locked magnetization from the solvent to the exchanging labile protons—hence preserving the efficiency of the $^1H\rightarrow{}^{15}N$ process—even if at the expense of substantially longer contact times than a conventional CP (a feature that is also shared by the BRAIN-CP experiment).

Figure 2 employs an alanine-based model to examine the resilience of the experiments depicted in Figure 1, in terms of their broadband-ness under conditions of slower and faster exchanges (298 and 333 K). These experiments were optimized so as to fulfill the HH demands and were measured as a function of the central ^1H carrier offset. Intensities in this and in all remaining plots of this study are shown normalized to the ^{15}N amplitude arising upon applying a DIPSI-2-based CP[22] at the highest available powers ($\gamma B_1/2\pi \approx 3.4$ and 3.1 kHz for the 498 MHz and 1 GHz NMR experiments respectively) and at 298 K, as this was considered the most robust and common scenario for conventional CP-based solution NMR transfers. In Figure 2a, the DIPSI scheme with $\gamma B_1/2\pi = 3.4$ kHz shows good sensitivity when applied at $\delta(^1H)\approx 6$–8 ppm, but it drops substantially as the offset moves away and water's spin-locking is lost. This drop becomes more severe as the spin-locking field decreases from 3.4 to 2.0 kHz. Also, MOIST variants are significantly degraded by the combined action of exchange plus ^1H off-resonance. By contrast, the novel L-WURST and TAPF-CP variants show high broadbandness —the former owing to its use of swept pulses, and the latter due to its stronger instantaneous $\gamma_H B_{1,H}$ fields. The use of WURST, in particular, allows one to extend the coverage all the way up to the 14 ppm region demanded by imino protons. Supporting Figure S1 extends these comparisons to data measured at other temperatures, where similar trends are observed. Unlike what happens when changing the ^1H offset, changing the ^{15}N offset over a standard chemical shift range makes little difference on the signals measured by these experiments except for MOIST-CP (Supporting Figure S2). It was also found that different cycle times and arrangements for the +x/-x alternation, make little difference in the overall performance of the TAPF-CP (data not shown). What did introduce a difference in the TAPF-CP performance was adding a linear ramp in the amplitude of the RF pulses, yet another provision commonly implemented in solid-state CP NMR.[27] For instance, it was found that by ramping the amplitude of the ^{15}N CW throughout a 10 % range of the nominal HH demands, alanine's TAPF-CP maximum signal intensity did not change—but the optimized contact time went from 400 ms in the constant amplitude case, to 240 ms in the ramped amplitude one. None of the other variants exhibited similar changes regarding signal intensity and/or optimal contact time with ramping. Amplitude ramping therefore appears beneficial to alleviate a potential complication of the TAPF sequence, related to its need for relatively long contact times.

The situation is both similar and different when comparing the various sequences at 1 GHz (Figure 2b). The CP efficiency of DIPSI is markedly better than all counterparts at lower temperatures, presumably thanks to its shorter contact times. However, the efficiencies of all sequences become significantly lower upon increasing temperature— even when compared to the efficiency drops measured at 498 MHz. We ascribe this to the loss of the water and H_N signals during the spin-lock period: for instance, a 20 % signal loss was observed for these ^1H resonances when applying L-WURST-CP at 1 GHz NMR over a 300 ms contact time, whereas negligible losses were observed in these peaks at the lower field. Particularly marked are the ca. 90 % losses exhibited by DIPSI-CP under these high-field, fast-exchange conditions. Such losses go beyond the aforementioned $T_{1\rho}$ effects. As nearly identical behaviors were observed when experiments were repeated under dematched or spatially-limited samples, these losses are unlikely to arise from radiation damping and/or RF inhomogeneity effects; we are investigating whether interferences between the exchange process and DIPSI's composite-

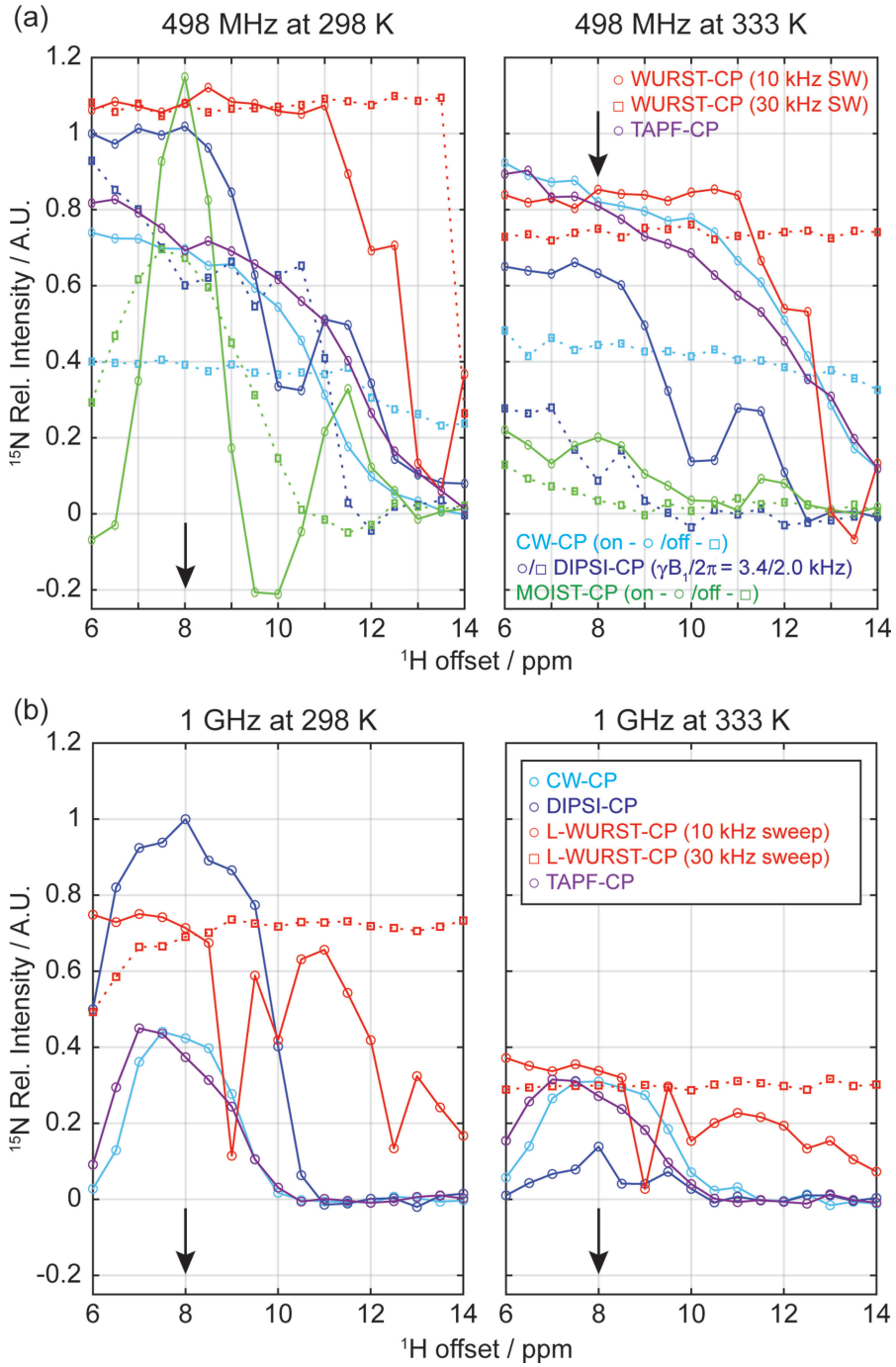

Figure 2. CP NMR excitation profiles measured as a function of the ^{1}H offset in ^{15}N-detected experiments on L-alanine's amino group at pH 2.1 at (a) 498 MHz and (b) 1 GHz. The resonance position of alanine is indicated by black arrows. Except for L-WURST-CP and TAPF-CP data, the RF fields of ^{15}N were 3.4 kHz in (a) and 3.1 kHz in (b); ^{1}H RF fields were chosen to match the HH conditions. The L-WURST-CP data was measured using two WURST pulses: one with 10 ms duration and 10 kHz sweep (red circle), the other of 30 ms duration and 30 kHz sweep (red square). In both cases the ^{1}H RF fields were 2.0 kHz. TAPF-CP was applied on-resonance with nutation fields of 10 kHz and 3.3 kHz in (a), and of 9.4 kHz and 3.1 kHz in (b), for the ^{1}H and ^{15}N channels, respectively. In (a), DIPSI-CP was also measured with a nutation field of 2.0 kHz (blue squares), and CW- and MOIST-based CP were assayed both on-resonance (circles, "on") and with the ^{15}N shifted $\Delta\Omega_N = 9.5$ and 5.0 kHz (190 and 100 ppm) off-resonance (squares, "off"), with HH conditions on the ^{15}N matched accordingly. All intensities are normalized to the maximum peak height measured with DIPSI-CP at 298 K. Optimal transfer times for (a) were 21–45 and 40–60 ms (DIPSI-CP using 2.0 kHz and 3.4 kHz), 140–220 ms (CW-CP), 8 ms (MOIST-CP), 180–200/360–540 ms (L-WURST-CP using 10 kHz/30 kHz sweep), and 140–400 ms (TAPF-CP). Optimal transfer times for (b) were 10–20 ms (DIPSI-CP), 60 ms (CW-CP), 120–160/180–360 ms (L-WURST-CP using 10 kHz/30 kHz sweep), and 80–100 ms (TAPF-CP). See Supporting Figure S3 for additional insight on the ^{15}N offset dependence of these experiments.

pulse cycle could explain them. By contrast, the new CP methods demonstrated relative resilience under these high-field, fast-exchanging conditions: as at lower fields, the L-WURST-CP showed then the best compromise between sensitivity and ^{1}H bandwidth.

Figure 3 uses the same L-alanine model to examine the resilience of the experiments depicted in Figure 1, against the effects of chemical exchange. These were evaluated by measuring ^{1}H→^{15}N polarization transfer efficiencies for alanine's ^{15}N signal in water as a function of temperature, within the RF and thermal limits of our cold probehead. At all exchange conditions, the INEPT performance is markedly poorer than that of all CP counterparts; these limitations become even more evident as temperature increases. All CP variants give similar performances at the lowest temperature when applied on-resonance on the 42 ppm ^{15}N signal; although going off-resonance in the ^{15}N channel enables the use of larger $B_{1,H}$ fields,[28,29] the overall CP performance tends to be poorer—probably as a result of the *sinθ* scaling brought about in the efficiency of the HH recoupling upon varying the $\theta = \tan^{-1}(\gamma_N B_{1,N}/\Delta\Omega_N)$ spin-locking axis. Also notable are the decreased performances of phase-alternating sequences like MOIST and DIPSI as exchange rates increase, perhaps reflecting interferences between stochastic exchange and coherent phase-shifting processes that begin to act on similar timescales.

As mentioned, a H^{water}→H^{N}→^{15}N "conveyor" of spin-locked magnetizations is important for enabling an efficient polarization transfer to the ^{15}N, despite the onset of fast chemical exchanges. Figure 4 explores this aspect of the CP process with three variants introduced in Figure 1, as clarified by Liouville-space simulations. These numerical calculations accounted for chemical exchange, spin relaxation, and RF waveforms centered on-resonance with the labile proton;[15] in addition, a 4 ppm offset between the H^{N} and the water resonance (498 MHz) was considered. The introduction of this offset, akin to that arising in alanine, drops the maximum achievable ^{15}N enhancement from the ≈100 % value arising in the absence of chemical shifts (Figure 7 in ref. [15]), to ca. 60 %. Importantly, the effects of the solvent exchange on the ^{15}N buildup are similar for all the pulse sequences, confirming the preservation of the water repolarization process—which adds to the broadband characteristics of the novel L-WURST-CP and TAPF-CP experiments illustrated above. Also visible in these plots are the rapid modulations introduced on the water by TAPF's phase switches, as well as the adiabatic inversions introduced by L-WURST-CP that continuously invert the proton magnetizations from +z to -z and back to +z. This becomes somewhat of a drawback when this approach is applied in the absence of exchange, as these inversions need to be then coordinated with the J-driven CP oscillations in order to maximize the effects of the H^{N} →^{15}N transfer. By smoothing the latter oscillations, the onset of solvent exchanges removes this need for a precise timing. Furthermore, although these simulations focus on two-spin systems, qualitatively similar considerations are expected to hold—even if with slightly modified contact times—for more complex NH_2 and NH_3 systems.

Figure 5 explores the efficiency of CP processes based on the DIPSI, L-WURST and TAPF variants, as applied to the direct ^{15}N detection of lysine side-chain in unfolded α-synuclein and in a drkN SH3 fragment under majority-folded conditions. All ^{1}H→^{15}N transfer experiments were

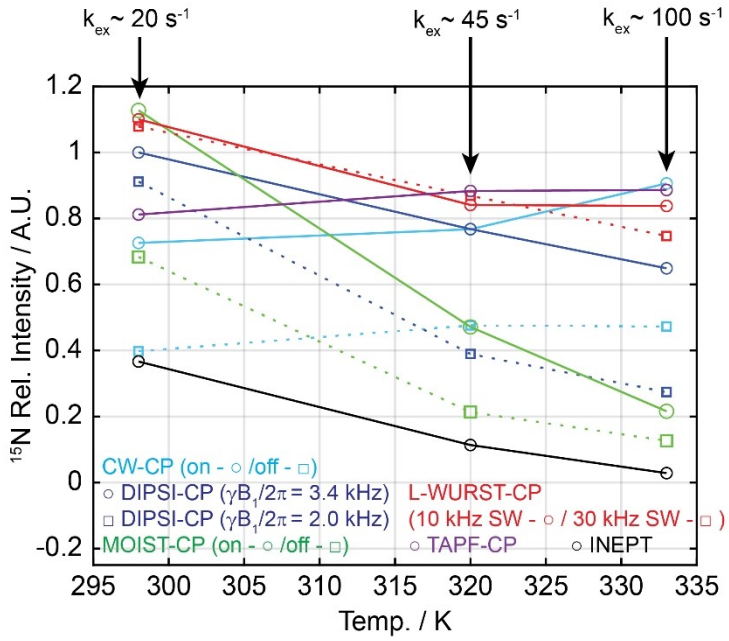

Figure 3. ^{15}N-detected CP experiments measured on L-alanine at pH 2.1 and at three different temperatures, using the indicated sequences (498 MHz NMR). Shown on top are the approximate solvent exchange rates of the ^{1}Hs serving as source of polarization, as estimated by ^{1}H line shape analyses. Other experimental conditions were as described for Figure 2a.

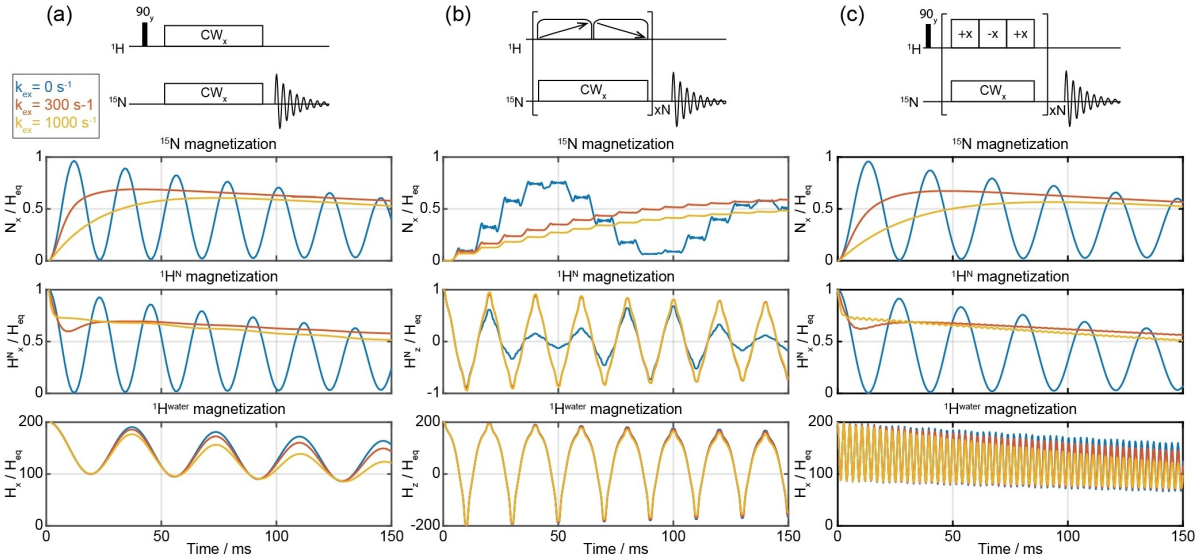

Figure 4. Liouville-space simulations for the performance of ^{1}H→^{15}N transfer plotted at different exchange rates. H^{N} and N are assumed irradiated on resonance, H^{water} is off resonance by 4 ppm. (a) Conventional CW-CP with the nutation field of 3.5 kHz. L-WURST-CP simulated with WURST pulses with a duration of 10 ms and sweep of 10 kHz. The nutation field is 3.5 kHz, and the number of loops is 8. (c) TAPF-CP with the nutation field of 10 kHz and 3.3 kHz for ^{1}H and ^{15}N, respectively. Each cycle contains 300 us duration of phase-alternating/constant phase spin-locking pulses on ^{1}H/^{15}N, respectively. All simulations were performed with the Spinach software package;[30] detailed simulation parameters are indicated in the Experimental section.

recorded at 498 MHz (^{1}H), and the former sample was examined at two temperatures. Lysine side chains were chosen as these residues are known for having fast solvent exchange rates ($k_{ex} \geq 100\ s^{-1}$).[33] ^{1}H→^{15}N transfers were thus explored in ^{15}N-labeled α-synuclein and in an ^{15}N-labeled fragment of SH3, containing a total of 14 and 5 lysine residues, respectively. These sidechains are also mobile, and hence only single resonances were observed in their 1D ^{15}N NMR spectra. The general behavior observed for the residues in these two proteins is very similar, with the rapid solvent exchanges precluding the observation of INEPT-derived signals but not of the CP counterparts. Somewhat along the lines displayed by the alanine data at 333 K, TAPF provides the highest transfer efficiency for these fast exchanging groups.

Novel CP strategies for polarizing ^{15}N sites bound to solvent exchanging protons should open possibilities for enhancing triple-resonance experiments involving transfers to ^{13}C that are J-coupled to the ^{15}N.[21,31] Demonstrations of such concatenated CP (CCP) blocks have been presented for both non-exchanging[32] and exchanging systems.[15] In such cases, the first CP is optimized for performing a ^{1}H→^{15}N transfer, and is followed by a second CP process implementing the ^{15}N→^{13}C transfer. Figure 6a shows pulse sequences adapted to test into CCP the performance of the novel CP blocks introduced in Figure 1; Figure 6b examines the resulting experiments when applied to ^{13}C/^{15}N-enriched urea, together with ^{1}H→^{15}N→^{13}C transfers based on conventional CP-CP and INEPT-INEPT (both of these refocused) sequences. These tests measured the carbonyl signal of this compound when placed in water, at three different temperatures. As expected from the ^{15}N measurements, the INEPT-based sequences show poor performance, while all CP-based ones provide detectable signals in all temperature ranges. In parallel to what was shown in Figure 3, CCP's efficiency decrease with temperature; a similar observation was reported by Lopez et al.,[34] whereby the intensity of CP-based HNCO experiments dropped as a function of temperature, but was always better than INEPT-based HNCO experiments. Notice how the new CP versions maintain their efficiency despite the onset of faster chemical exchanges at higher-temperatures. Similar experiments were used to target the lysine side chains of PhoA4, an intrinsically disordered protein. These sidechains are mobile and, in parallel with what was noticed in the ^{15}N-detected experiments, basing the initial CP on TAPF provided the best sensitivity among all CCP variants. Supporting Figure S4 presents additional results obtained upon applying these CCP strategies to enhance the carbonyl region signals of two IDPs, via polarization transfers starting from the amide protons. While also here CCP shows better efficiency than INEPT-based counterparts at all temperatures, the heterogeneous nature of the samples makes a detailed interpretation more challenging than in the cases introduced in Figure 6: in many instances slowly-exchanging residues provide the DIPSI-based transfer with the best sensitivity; however, this sequence's deterioration with increasing temperatures is clearly more marked than those of the L-WURST and TAPF variants.

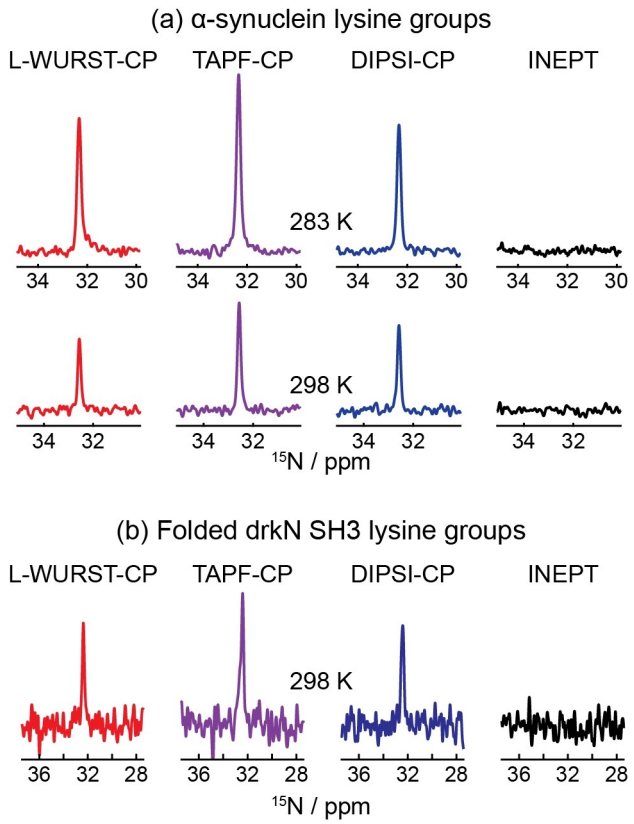

Figure 5. Detecting lysine's side-chain $^{15}N^{\zeta}$ signal by CP in (a) α-synuclein and (b) folded drkN SH3, respectively. For both proteins the nutation field for the $^{1}H\rightarrow^{15}N$ transfer was as indicated in Figure 2, and temperatures were as indicated in this Figure. The CP contact times of $^{1}H\rightarrow^{15}N$ transfers in (a) were 80/170 ms (DIPSI-2), 240/320 ms (WURST-CP), and 110/300 ms (TAPF-CP), with the different times corresponding to the two different temperatures. For (b), contacts were 240 ms (L-WURST-CP), 200 ms (TAPF-CP, used ramped CW for ^{15}N), and 120 ms (DIPSI-CP) respectively. No signals were detected for any protein sample when performing refocused INEPT experiments. See Experimental methods for further details. In all cases the ^{15}N RF was centered on-resonance with the single lysine peak detected; central ^{1}H offsets were scanned between 5.5 and 9 ppm and in parked at the position of maximum transfer efficiency (≈6 ppm).

Conclusion

CP-based experiments are generally superior to INEPT-based counterparts when targeting labile protons, This is thanks to additional exchange-driven polarization $H^{water}\rightarrow H^{N}$ transfers, that will allow the primary $H^{N}\rightarrow N^{x}$ transfer to proceed. Taking advantage of these chemical exchanges requires ensuring a simultaneous spin-locking of both the H^{N} and H^{water} magnetizations, something which is difficult to achieve while under Hartmann-Hahn matching due to the limited $\gamma_N B_{1,N}$ fields available. The present study examined schemes that can provide broad ^{1}H effective spin-locks covering wider chemical shift ranges, even while fulfilling the ^{15}N-imposed HH match. The simplest option involved adding an off-resonance onto the ^{15}N, leading to larger $\sqrt{(\gamma_N B_{1,N})^2+\Delta\Omega_N}$ effective fields, and hence to the possibility of utilizing the extra power available in the ^{1}H RF channel. This route proved disappointing, both when confronted with ^{1}H off-resonance effects and with rapid chemical exchanges. Alternatives were thus sought in solid-state NMR experiments; in particular on schemes relying on adiabatic pulses that will perform spin-locking over a range of offsets defined by their sweep ranges, and on time-alternated phase-flipped schemes that will match strong $\gamma_H B_{1,H}$ fields to lower $\gamma_N B_{1,N}$ fields on an "average" sense. These alternatives showed improvements vis-à-vis CW- or DIPSI-based CP schemes, both in terms of the range of operational ^{1}H offsets, and of resilience to chemical exchanges. Their performance, however, is still far from optimal in a number of aspects. One is still a limited chemical shift range; indeed, though expanded, the TAPF range is still insufficient to cover imino protons resonating at ca. 14 ppm. This range—and even wider ones—can be easily covered by the L-WURST-CP, but the efficiency per unit time of this sequence is limited, necessitating multiple loops and, in turn, long contact times for its operation. Still, these new solids-inspired schemes seem to present improved solutions to this long-standing problem, providing broad-banded ^{1}H effective fields which can potentially be applied to numerous double and triple resonance experiments involving fast exchanging labile protons at physiological conditions.

Acknowledgements

We are grateful to Profs. I. Kuprov, P. Selenko and to Dr. M. Jaroszewicz for valuable discussions. JK and JTG were supported by the Israel Academy of Sciences and Humanities & Council for Higher Education Excellence Fellowship Program for International Postdoctoral Researchers. LF holds the Bertha and Isadore Gudelsky Professorial Chair and Heads the Clore Institute for High-Field Magnetic Resonance Imaging and Spectroscopy, whose support is acknowledged. This work was supported by Israel Science Foundation Grants 1874/22 and 2790/22, the Perlman Family Foundation, and the EU Horizon 2020 program (FET-OPEN Grant 828946, PATHOS).

Conflict of Interest

The authors declare no conflict of interest.

Data Availability Statement

The data that support the findings of this study are available from the corresponding author upon request.

Keywords: Adiabatic Sweeps · Chemical Exchange · Cross Polarization · INEPT · Intrinsically Disordered Proteins

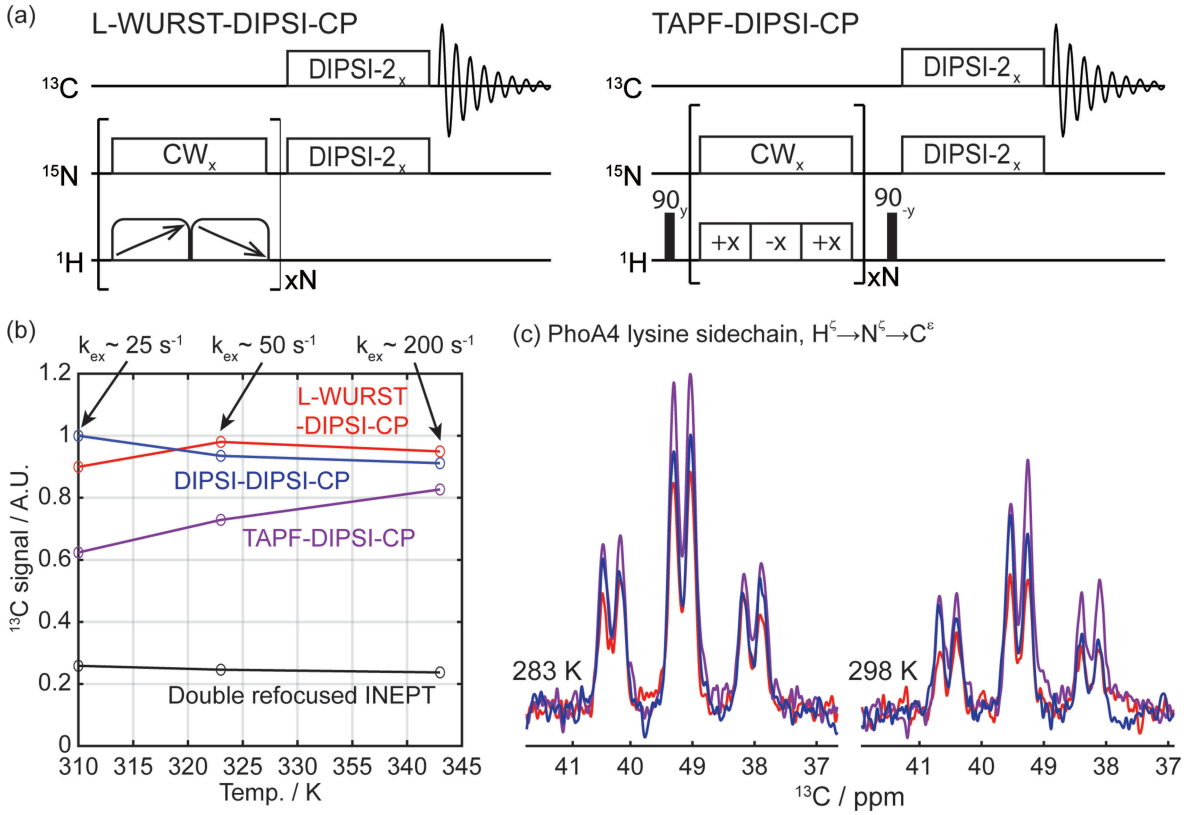

Figure 6. (a) Pulse sequences of WURST-DIPSI-CP and TAPF-DIPSI-CP for $H^N \rightarrow N^H \rightarrow C$ polarization transfer. (b) Carbonyl ^{13}C signals measured on urea sample at three different temperatures, normalized by DIPSI-DIPSI results at 310 K. Indicated as well are approximate rates of solvent exchange, as estimated from line shape analyses. (c) Detecting lysine's side-chain $^{13}C^{\varepsilon}$ signals by CCP experiments in PhoA4. The nutation fields used for these $^1H \rightarrow ^{15}N$ transfers were the same as in the alanine case shown in Figure 2, but CP contact times were optimized for maximum signal. These optimal CP contact times were: 10–40 ms (DIPSI-based CCP), 240–260 ms (L-WURST-based CCP), and 430–500 ms (TAPF-based CCP) for urea in the 310–343 K temperature range; 90/110 ms (DIPSI-based CCP), 280/320 ms (L-WURST-based CCP), 165/300 ms (TAPF-based CCP) for PhoA4 at 283 and 298 K, respectively. The duration and matched nutation fields for the N→C transfer were 28 ms and 1500 Hz for urea; 125/150 ms and 1250 Hz for PhoA4. The multiplicity of the $^{13}C^{\varepsilon}$ signals in (c) reflects the J-coupling between $^{13}C^{\varepsilon}$ and $^{13}C^{\delta}$ (~35 Hz) and between $^{13}C^{\varepsilon}$ and ^1H (~140 Hz); the splitting arising from the $^{13}C^{\varepsilon}$-$^{15}N^{\zeta}$ J-coupling (~5 Hz) is too small to be seen in these spectra. Note that no signals were detected for PhoA4 protein when performing ^{13}C-detected experiments based on $^1H \rightarrow ^{15}N$ INEPT transfers. Evolution times for the double-refocused INEPT blocks were optimized at each temperature to reach the maximum signal.

[1] W. P. Aue, E. Bartholdi, R. R. Ernst, *J. Chem. Phys.* **1976**, *64*, 2229–2246.
[2] K. Nagayama, K. Wüthrich, P. Bachmann, R. R. Ernst, *Naturwissenschaften* **1977**, *64*, 581–583.
[3] A. A. Maudsley, R. R. Ernst, *Chem. Phys. Lett.* **1977**, *50*, 368–372.
[4] G. A. Morris, R. Freeman, *J. Am. Chem. Soc.* **1979**, *101*, 760–762.
[5] L. Mueller, *J. Am. Chem. Soc.* **1979**, *101*, 4481–4484.
[6] M. Sattler, J. Schleucher, C. Griesinger, *Prog. Nucl. Magn. Reson. Spectrosc.* **1999**, *34*, 93–158.
[7] G. Varani, F. Aboul-ela, F. H.-T. Allain, *Prog. Nucl. Magn. Reson. Spectrosc.* **1996**, *29*, 51–127.
[8] B. Fürtig, C. Richter, J. Wöhnert, H. Schwalbe, *ChemBioChem* **2003**, *4*, 936–962.
[9] G. Bodenhausen, D. J. Ruben, *Chem. Phys. Lett.* **1980**, *69*, 185–189.
[10] R. D. Bertrand, W. B. Moniz, A. N. Garroway, G. C. Chingas, *J. Am. Chem. Soc.* **1978**, *100*, 5227–5229.
[11] G. C. Chingas, A. N. Garroway, W. B. Moniz, R. D. Bertrand, *J. Am. Chem. Soc.* **1980**, *102*, 2526–2528.
[12] M. Ernst, C. Griesinger, R. R. Ernst, W. Bermel, *Mol. Phys.* **1991**, *74*, 219–252.
[13] P. Pelupessy, E. Chiarparin, *Concepts Magn. Reson.* **2000**, *12*, 103–124.
[14] T. Parella, *J. Biomol. NMR* **2004**, *29*, 37–55.
[15] M. Novakovic, S. Jayanthi, A. Lupulescu, M. G. Concilio, J. Kim, D. Columbus, I. Kuprov, L. Frydman, *J. Magn. Reson.* **2021**, *333*, 107083.
[16] T. Yuwen, N. R. Skrynnikov, *J. Biomol. NMR* **2014**, *58*, 175–192.
[17] S. R. Hartmann, E. L. Hahn, *Phys. Rev.* **1962**, *128*, 2042–2053.
[18] M. J. Duer, *Introduction to Solid-State NMR Spectroscopy*, Blackwell Science, Oxford, **2008**.
[19] D. E. Demco, J. Tegenfeldt, J. S. Waugh, *Phys. Rev. B* **1975**, *11*, 4133–4151.
[20] B. H. Meier, *Chem. Phys. Lett.* **1992**, *188*, 201–207.
[21] I. C. Felli, R. Pierattelli, *J. Magn. Reson.* **2014**, *241*, 115–125.
[22] S. P. Rucker, A. J. Shaka, *Mol. Phys.* **1989**, *68*, 509–517.
[23] M. H. Levitt, *J. Chem. Phys.* **1991**, *94*, 30–38.
[24] K. Takegoshi, C. A. McDowell, *J. Magn. Reson. 1969* **1986**, *67*, 356–361.
[25] K. J. Harris, A. Lupulescu, B. E. G. Lucier, L. Frydman, R. W. Schurko, *J. Magn. Reson.* **2012**, *224*, 38–47.

[26] E. Kupce, R. Freeman, *J. Magn. Reson. Ser. A* **1995**, *115*, 273–276.
[27] G. Metz, M. Ziliox, S. O. Smith, *Solid State Nucl. Magn. Reson.* **1996**, *7*, 155–160.
[28] A. Bax, B. L. Hawkins, G. E. Maciel, *J. Magn. Reson. 1969* **1984**, *59*, 530–535.
[29] S. C. Shekar, D.-K. Lee, A. Ramamoorthy, *J. Am. Chem. Soc.* **2001**, *123*, 7467–7468.
[30] H. J. Hogben, M. Krzystyniak, G. T. P. Charnock, P. J. Hore, I. Kuprov, *J. Magn. Reson.* **2011**, *208*, 179–194.
[31] W. Bermel, I. Bertini, I. C. Felli, M. Piccioli, R. Pierattelli, *Prog. Nucl. Magn. Reson. Spectrosc.* **2006**, *48*, 25–45.
[32] A. Majumdar, E. R. P. Zuiderweg, *J. Magn. Reson. Ser. A* **1995**, *113*, 19–31.
[33] J. Iwahara, Y.-S. Jung, G. M. Clore, *J. Am. Chem. Soc.* **2007**, *129*, 2971–2980.
[34] J. Lopez, R. Schneider, F.-X. Cantrelle, I. Huvent, G. Lippens, *Angew. Chem. Int. Ed.* **2016**, *55*, 7418–7422.

Manuscript received: April 6, 2023
Accepted manuscript online: July 5, 2023
Version of record online: July 5, 2023